THIS THESIS IS

DEVOTED TO MY

CHERISHED PARENTS, UNCLE AND SIBLINGS

AS WELL AS

MY MENTORS

IN APPRECIATION OF THEIR UNWAVERING INSPIRATION, WHOLEHEARTED SUPPORT, AND INVALUABLE GUIDANCE

DrillBit

The Report is Generated by DrillBit Plagiarism Detection Software

Submission Information

Author Name	Modhusudan Mondal
Title	EXPLORATION OF DIVERSE INTERACTIONS OF SOME SIGNIFICANT COMPOUNDS PREVAILING IN HOST GUEST INCLUSION COMPLEXES AND SOLUTION CHEMISTRY IN VARIOUS ENVIRONMENTS FOR ADVANCED APPLICATIONS BY PHYSICOCHEMICAL CONTRIVANCE
Paper Submission ID	2144597
Submitted by	nbuplg@nbu.ac.in
Submission Date	2024-07-22 11:06:43
Total Pages, Total Words	262, 59959
Document type	Thesis

Result Information

Similarity **0 %**

Exclude Information

Quotes	Excluded
References/Bibliography	Excluded
Source: Excluded < 14 Words	Excluded
Excluded Source	**6 %**
Excluded Phrases	Not Excluded

Database Selection

Language	English
Student Papers	Yes
Journals & publishers	Yes
Internet or Web	Yes
Institution Repository	Yes

A Unique QR Code use to View/Download/Share Pdf File

Modhusudan Mondal

Signature of the Candidate

Malendra Nath Roy (26-07-2024)

Signature of the Principal Supervisor

Prof. (Dr.) M. N. Roy
FRSC (London), UK
Department of Chemistry
University of North Bengal
Darjeeling-734013, India

Kanak Roy

Signature of the Co-Supervisor

Assistant Professor
Department of Chemistry
Alipurduar University,
Alipurduar -736122, India

UNIVERSITY OF NORTH BENGAL

PROF. (DR.) M. N. ROY

FRSC (London)

Professor of Chemistry and Dean of Science and Arts, Commerce and Law, NBU and Founder Vice-Chancellor of Alipurduar University

Awardee of One Time Grant from UGC, Prof. Suresh C. Ameta Award from ICS, Bronze Medal from CRSI

Shiksha Ratna, Dooars Ratna and Banga Bhushan from the Government of West Bengal

and

Bharat Siksha Award and C V Raman Prize from the Government of India

समानो मन्त्रः समितिः समानी

Phone : 0353 2776381
Mobile: 094344 96154
Fax: +91 353 2699001

Darjeeling-734 013,
West Bengal, INDIA

July 26, 2024

E-mail:
mahendraroy2002@yahoo.co.in/
mahendraroy2018@nbu.ac.in

CERTIFICATE

I, certify that Mr. Modhusudan Mondal has prepared his thesis entitled "EXPLORATION OF DIVERSE INTERACTIONS OF SOME SIGNIFICANT COMPOUNDS PREVAILING IN HOST GUEST INCLUSION COMPLEXES AND SOLUTION CHEMISTRY IN VARIOUS ENVIRONMENTS FOR ADVANCED APPLICATIONS BY PHYSICOCHEMICAL CONTRIVANCE", for the award of **Ph.D. Degree (Doctor of Philosophy)** from the University of North Bengal, under our guidance. He has carried out his work at the Department of Chemistry, University of North Bengal. The contents of this thesis, in full or in parts, have not been submitted to any other Institution or University for the award of any degree or diploma.

Mahendra Nath Roy (26-07-2024)

PROF. (DR.) MAHENDRA NATH ROY

Department of Chemistry,
University of North Bengal,
Darjeeling: 734013,
West Bengal, India
DATE:

Prof. (Dr.) M. N. Roy
FRSC (London), UK
Department of Chemistry
University of North Bengal
Darjeeling-734013, India

ALIPURDUAR UNIVERSITY
(ERSTWHILE ALIPURDUAR COLLEGE)

Dr. Kanak Roy, M.Sc, B.Ed, Ph.D
Assistant Professor
Department of Chemistry

P.O.: Alipurduar Court, Alipurduar,
West Bengal, India, Pin:736122
Tel. Phone: 03564-255046
Mobile: +919735996366
E-mail: kanakroynbu@gmail.com

CERTIFICATE

I certify that Mr. Modhusudan Mondal has prepared the thesis entitled **"EXPLORATION OF DIVERSE INTERACTIONS OF SOME SIGNIFICANT COMPOUNDS PREVAILING IN HOST GUEST INCLUSION COMPLEXES AND SOLUTION CHEMISTRY IN VARIOUS ENVIRONMENTS FOR ADVANCED APPLICATIONS BY PHYSICOCHEMICAL CONTRIVANCE"** for the award of **Ph.D. (Doctor of Philosophy)** degree of the University of North Bengal, under our guidance. He has carried out the research work at the Department of Chemistry, University of North Bengal.

Kanak Roy

DR. KANAK ROY
(Co-Supervisor)
Assistant Professor
Department of Chemistry
Alipurduar University
Alipurduar, 736122
West Bengal, India

Assistant Professor
Department of Chemistry
Alipurduar University,
Alipurduar -736122, India

Date: 26.07.2024

DECLARATION

I, Modhusudan Mondal, declare that the thesis entitled "EXPLORATION OF DIVERSE INTERACTIONS OF SOME SIGNIFICANT COMPOUNDS PREVAILING IN HOST GUEST INCLUSION COMPLEXES AND SOLUTION CHEMISTRY IN VARIOUS ENVIRONMENTS FOR ADVANCED APPLICATIONS BY PHYSICOCHEMICAL CONTRIVANCE" has been prepared by me for the Degree of **Doctor of Philosophy (Ph.D.)** under the supervision of **Dr. Mahendra Nath Roy, FRSC (London), (Principal Supervisor)**, Professor of Chemistry, University of North Bengal and Dr. Kanak Roy (Co-Supervisor), Asst. Professor of Chemistry, Alipurduar University. No part of this thesis has formed the basis for the award of any other degree or diploma, in this or any other Institution or University.

Modhusudan Mondal.

MR. MODHUSUDAN MONDAL
Department of Chemistry
University of North Bengal
Darjeeling: 734013
West Bengal, India

Date: 26-07-2024.

ACKNOWLEDGEMENT

Every success is a journey filled with remarkable adventures and unforgettable experiences. I am profoundly grateful to all those who have supported me throughout this incredible journey.

First and foremost, I extend my heartfelt thanks and praise to the Almighty God for guiding me through my research and providing the resources necessary to complete it.

I am deeply thankful to my esteemed supervisor, Dr. Mahendra Nath Roy, FRSC (London), Professor of Chemistry at the University of North Bengal, West Bengal, India. His unwavering guidance, insightful advice, and inspiration were instrumental throughout my research. His trust in me and the freedom to explore my ideas made me feel truly blessed and honored to complete my thesis under his mentorship. This study would not have been possible without his persistent support, responsible direction, and invaluable supervision. Thank you, sir, for treating me like family and providing a nurturing environment.

My sincere gratitude extends to my co-supervisor, Dr. Kanak Roy, Assistant Professor in the Department of Chemistry at Alipurduar University, Alipurduar, West Bengal, India. His invaluable assistance, constant support, and encouragement greatly aided the completion of this study.

I am also deeply appreciative of Prof. (Dr.) Bhaskar Biswas, the honorable Head of the Department of Chemistry at NBU, for his thorough advice and guidance throughout the study process.

I wish to express my heartfelt thanks to the faculty members, officers, and academic staff of the Department of Chemistry at the University of North Bengal for their valuable assistance and ongoing inspiration. I am grateful to the university for providing lab facilities, especially USIC and NBU, which offered access to essential instrumentation.

I would like to extend my deepest gratitude to my collaborators for their invaluable contributions and unwavering support throughout my research journey.

A special note of appreciation goes to Miss Shatarupa Basak, my lab partner since my college days, for her invaluable help, advice, unwavering encouragement, and motivation during my research.

I would like to express my profound gratitude to Dr. Subhadeep Saha, Mr. Salim Ali, Dr. Biplab Rajbanshi, Dr. Narendra Nath Ghosh, Dr. Subhankar Choudhury, Mr. Salman Haydar, Dr. Biswajit Ghosh, Dr. Pranish Bomzan, Dr. Niloy Roy, and Mr. Subhajit Debnath for their invaluable assistance, advice, and collaboration throughout my research. Additionally, I thank all my junior lab mates, including Baishali, Sanjoy, Ayesha, Ajit, Priyanka, Kangkan, Doli, Mantu, and others, for creating a homely environment and supporting me throughout my research career, making the completion of this work possible.

I extend my heartfelt gratitude to my beloved parents, Mr. Montu Mondal and Mrs. Monju Mondal, whose limitless love, care, prayers, and sacrifices have played a crucial role in my education and personal growth. I am also profoundly appreciative of my dear uncle, Mr. Bimal Chandra Mandal, and aunt, Mrs. Rita Mandal, for their steadfast support, prayers, and sacrifices in nurturing and preparing me for my future.

I outspread my heartfelt appreciation to my grandfathers, the Late Kiran Chandra Mondal and Nani Bala Mondal, and my grandmothers. I owe a great deal of gratitude to my sisters, Mrs. Dipali Mondal, Mrs. Shefali Biswas, Mrs. Shyamali Majumder, and Miss Shilpi Mandal for their motivation and assistance in completing my research. My heartfelt thanks also go to my only brother, Manoj Mandal, for his support and help in preparing me for the future.

Additionally, I am sincerely grateful to my other uncles, Mr. Nirod Mandal and Mr. Nikhil Mondal; my aunties, Mrs. Anna Mandal and Mrs. Dipali Mondal; and my other siblings, Mr. Nirmal Mondal, Mrs. Kasturi Guin (sister-in-law), Mrs. Anima Mondal, Nimai, Abhijit, Tumpa, Narayan, Priyanka, Sayantika, Ritesh, and others. Their countless blessings, well-wishes, and dedication to supporting my goals have shaped who I am today and who I will become in the future.

I also want to convey my heartfelt thanks to my friends cum brothers Kaushik Da, Shashanka Da, Pranay Da, Milton, Debashis, Papiya, Rana, Bidyut, Balaram, Naru, Biswo, Gautam, Kumaresh, Sasmal, Sanjoy, Prasnata, Modi and others for their companionship, which kept me stress-free.

I wish to acknowledge all my esteemed teachers from Nandajhar A.T High School, Islampur High School, Malda College, and the University of North Bengal, as well as tutors from different institutions. The knowledge and guidance they imparted have been invaluable in enabling me to conduct my research work successfully.

Special thanks go to the editors, co-editors, and reviewers of my articles for their constructive criticism and suggestions, which were instrumental in conducting my research. I respectfully thank the writers and researchers of all the cited references, as their work provided the foundational information necessary for the development of new ideas.

Finally, I am grateful to the University Grants Commission (UGC) for their Junior Research Fellowship, reference number 191620113448, which provided the financial support needed to complete my research. I appreciate the advanced instrumental facilities available under the UGC's Special Assistance Programme Departmental Research Support-III (SAP-DRS-III). Additionally, I acknowledge the 'ONE TIME GRANT' Ref No. F.4-10/2010(BSR) awarded to my supervisor, Prof. (Dr.) Mahendra Nath Roy, through Basic Scientific Research (BSR), UGC, New Delhi, for financial and material support for my research projects. I also recognize SAIF-COCHIN, SAIF-IITM, SAIF-LPU, and SAIF-PANJAB for providing instrumental facilities.

Modhusudan Mondal

Mr. Modhusudan Mondal,

Department of Chemistry,

University of North Bengal,

Darjeeling: 734013,

West Bengal, India

DATE: 26-07-2024.

PREFACE

The research on the thesis titled "EXPLORATION OF DIVERSE INTERACTIONS OF SOME SIGNIFICANT COMPOUNDS PREVAILING IN HOST GUEST INCLUSION COMPLEXES AND SOLUTION CHEMISTRY IN VARIOUS ENVIRONMENTS FOR ADVANCED APPLICATIONS BY PHYSICOCHEMICAL CONTRIVANCE" began approximately five years ago, supervised by Prof. (Dr.) Mahendra Nath Roy, a senior Professor of Chemistry at the University of North Bengal and and Dr. Kanak Roy (Co-Supervisor), Asstistant Professor of Chemistry, Alipurduar University.

The project focuses on investigating the supramolecular host-guest inclusion complexation of various biologically active significant molecules, such as small drug molecules, dyes, and pollutants. The objective is to enhance their solubility and bioavailability. Additionally, the aim is to develop a drug delivery system for a promising water-soluble drug by utilizing inclusion complexes, enabling controlled release of the drug to the affected site without altering its chemical structure. Furthermore, the project also explores the interactions between amino acids and drugs in aqueous environments related to solution thermodynamics research.

During my research, I had the privilege of participating in several conferences and seminars throughout the country, where I had the opportunity to interact and learn from distinguished specialists and scientists. Moreover, I was fortunate enough to have my work related to the thesis published in a reputable international journal.

Whenever referring to the findings of other researchers, appropriate acknowledgement was given following the standard procedure for reporting scientific observations. I take full responsibility for any unintentional mistakes or oversights that may have occurred, despite taking precautions.

My objective is to encounter more challenges in life so that I can apply the knowledge and skills gained from my profession to real-world situations.

LIST OF TABLES

CHAPTERS	TABLES	PAGE NO.
CHAPTER IV	Table 1. Details of Name, Source, molecular weight, CAS Number and Mass Fraction of studied materials.	86
	Table 2. Chemical shift Data (in ppm) of protons of α-CD and β-CD in Free State and during IC formation with TZ.	86
	Table 3. Chemical shift Data (in ppm) of protons of TZ in Free State and during IC formation with CDs.	87
	Table 4. At 298.15 K, the surface tension (γ) values at the break point and the corresponding CD and Tartrazine concentrations.	87
	Table 5. At 298.15 K, the conductance values at the break point and the corresponding CD and Tartrazine concentrations.	87
	Table 6. Values of Association Constant (Ka) and Gibbs energy change (ΔG0) of the two systems (TZ-α-CD) and (TZ-β-CD).	88
	Table 7. CT-DNA binding constant for different systems.	88
	Table 8. Percentage of Degradation of Pure TZ, TZ-α-CD and TZ-β-CD under Fenton and Photo-Fenton processes.	88
	Table 9. Adsorption energies; HOMO, LUMO levels and band gap for (a) TZ-α-CD and (b) TZ-β-CD inclusion complexes.	88
	Table 10. ΔH° (kJ/mol); ΔG° (kJ/mol) and ΔS° (kJ/K) for (a) TZ-α-CD and (b) TZ-β-CD inclusion complexes in water medium.	89
	Table S1. Frequencies at FTIR spectra of TZ, α-CD, β-CD and ICs.	89-90
	Table S2. Data for the Job plot performed by UV-Vis spectroscopy for TZ+α-CD system at 298.15K[a].	91

CHAPTERS	TABLES	PAGE NO.
	Table S3. Data for the Job plot performed by UV-Vis spectroscopy for TZ+β-CD system at 298.15K[a].	91-92
	Table S4. Data for the surface tension study of TZ+α-CD system (concentration of stock solution of TZ= 10 mM, concentration of stock solution of α-CD = 10 mM) at 298.15K[a].	92
	Table S5. Data for the surface tension study of TZ+β-CD system (concentration of stock solution of TZ = 10 mM, concentration of stock solution of β-CD = 10 mM) at 298.15K[a].	93
	Table S6. Data for the conductivity study of TZ+αCD system (concentration of stock solution of TZ = 10 mM, concentration of stock solution of α-CD = 10 mM) at 298.15K[a].	94
	Table S7. Data for the conductivity study of TZ+β-CD system (concentration of stock solution of TZ = 10 mM, concentration of stock solution of β-CD = 10 mM) at 298.15K[a].	95
	Table S8. Data for the Benesi-Hildebrand double reciprocal plot performed by UV-Vis spectroscopy for TZ+α-CD system.	96
	Table S9. Data for the Benesi-Hildebrand double reciprocal plot performed by UV-Vis spectroscopy for TZ+β-CD system.	96
	Table 1: The surface tension (γ) values at the break point and the corresponding β-CD and 6-MP concentrations.	130
	Table 2: Values of Association Constant (K_a) and free energy change (ΔG^0) of the (6-MP-β-CD system.	130
	Table 3: Encapsulation Efficiency (EE%) β-CD inclusion ability toward 6-MP.	130
	Table 4: Chemical shift Data (in ppm) of protons of β-CD in Free State and during IC formation with 6-MP.	130

CHAPTERS	TABLES	PAGE NO.
CHAPTER V	**Table 5:** Chemical shift Data (in ppm) of protons of 6-MP in Free State and during IC formation with β-CD.	131
	Table 6: Aqueous solubility of 6-MP and 6-MP+β-CD at 25 ^{0}C.	131
	Table 7: CT-DNA binding constant for different systems.	131
	Table 8: Zone of inhibition observed against different bacteria (Data represented as mean ± SD of triplicate determination).	131
	Table S1: Descriptions of the Chemicals used in the work.	131-132
	Table S2: Data for the Job plot performed by UV-Vis spectroscopy for 6-MP+*β*-CD system at 298.15K^{a}.	132
	Table S3: Data for the surface tension study of 6-MP+*β*-CD system (concentration of stock solution of 6-MP = 10mM, concentration of stock solution of *β*-CD = 10mM) at 298.15K^{a}.	132-133
	Table S4: Data for the Benesi-Hildebrand double reciprocal plot performed by UV-Vis spectroscopy for 6-MP+*β*-CD system.	133-134
	Table S5: Frequencies at FTIR spectra of 6-MP, β-CD and IC.	134
CHAPTER VI	**Table 1:** Chemical shifts data (in ppm) of various protons in the free state of BPA and β-CD and its IC.	160
	Table 2: Different parameters obtained from *in silico* studies.	160
	Table 3: DPPH, ABTS, superoxide scavenging, FRAP and metal chelation activity of inclusion complex (IC) in comparison to bisphenol A (BPA) (results were expressed as average ± standard deviation of triplicate determinations).	161
	Table S1: Descriptions of the Chemicals used in the work.	161
	Table S2: Data for the Job plot performed by UV-Vis spectroscopy for BPA+*β*-CD system at 298.15K^{a}.	161-162

CHAPTERS	TABLES	PAGE NO.
	Table S3: Data for the Benesi-Hildebrand double reciprocal plot performed by UV-Vis spectroscopy for BPA+β-CD system.	162
	Table 1. At 298.15 K, Conductance and surface tension values at the break point and the corresponding CD and Dyphylline concentrations.	196
	Table 2. Values of Association Constant (K_a) and free energy change (ΔG^0) of the (Dyphylline-β- CD).	196
	Table 3. Change in chemical shifts (ppm) of different protons of the Dyphylline and β-CD when complexed with each other at 298.15 K.	196-197
	Table 4. Apparent molar volume ($\phi_V{}^0$), viscosity-*B* and viscosity-*A* co-efficient and Molar Refraction ($R_M{}^0$) of (BCD + DYPHYLLINE + H_2O) system in aqueous β-CD solutions of mass fractions, w_1 = 0.001, 003, 0.005 at temperatures 298.15 K, 303.15 K and 308.15 K.	197
	Table 5. Values of various coefficients of equation-6 for Dyphylline in three different mass fractions (w_1) of aqueous β-CD mixtures at three different temperatures.	198
	Table 6. Limiting apparent molar expansibility ($\phi_E{}^0$) for Dyphylline in three different mass fractions (w_1) of aqueous β-CD mixtures at three different temperatures.	198
	Table 7. Values of ($\bar{V}_1{}^0$–$\bar{V}_2{}^0$), $\Delta\mu_1{}^{0\neq}$, $\Delta\mu_2{}^{0\neq}$, $T\Delta S_2{}^{0\neq}$ and $\Delta H_2{}^{0\neq}$for Dyphylline in three different mass fractions (w_1) of aqueous β-CD mixtures at three different temperatures.	198-199
	Table 8. Zone of inhibition of tested samples against different bacteria studied (Data was represented as Mean ±SD of triplicate determination).	199
	Table S1. Descriptions of the Chemical used in the work.	200

CHAPTERS	TABLES	PAGE NO.
CHAPTER VII	**Table S2.** Data for the conductivity study of Dyphylline+β-CD system (concentration of stock solution of Dyphylline = 10 mM, concentration of stock solution of β-CD = 10 mM) at 298.15 K[a].	200
	Table S3. Data for the surface tension study of Dyphylline+β-CD system (concentration of stock solution of Dyphylline = 10 mM, concentration of stock solution of β-CD = 10 mM) at 298.15 K[a].	201
	Table S4. Data for the Job plot performed by UV-Vis spectroscopy for Dyphylline+β-CD system at 298.15 K[a].	202
	Table S5. Data for the Benesi-Hildebrand double reciprocal plot performed by UV-Vis spectroscopy for Dyphylline+β-CD system.	202
	Table S6. Density (ρ), Viscosity (η), Refractive index (n_D) of aqueous pure β-CD solutions of mass fractions, W_1 = 0.001, 003, 0.005 at temperatures 298.15 K, 303.15 K and 308.15 K.	203
	Table S7. Density (ρ), Viscosity (η), Refractive index (n_D) of aqueous pure (Dyphylline + β-CD + H_2O) system in aqueous β-CD solutions of mass fractions, W_1 = 0.001 at temperatures 298.15 K, 303.15 K and 308.15 K.	203-204
	Table S8. Density (ρ), Viscosity (η), Refractive index (n_D) of aqueous pure (Dyphylline + β-CD + H_2O) system in aqueous β-CD solutions of mass fractions, W_1 = 0.003 at temperatures 298.15 K, 303.15 K and 308.15 K.	204-205
	Table S9. Density (ρ), Viscosity (η), Refractive index (n_D) of aqueous pure (Dyphylline + β-CD + H_2O) system in aqueous β-CD solutions of mass fractions, W_1 = 0.005 at temperatures 298.15 K, 303.15 K and 308.15 K.	205-206

CHAPTERS	TABLES	PAGE NO.
	Table S10. Apparent molar volume (ϕ_V), (η_r-1)/$\sqrt{c}$ and Molar Refraction (R_M) of aqueous pure (Dyphylline + β-CD + H_2O) system in aqueous β-CD solutions of mass fractions, W_1 = 0.001 at temperatures 298.15 K, 303.15 K and 308.15 K.	206-207
	Table S11. Apparent molar volume (ϕ_V), (η_r-1)/$\sqrt{c}$ and Molar Refraction (R_M) of aqueous pure (Dyphylline + β-CD + H_2O) system in aqueous β-CD solutions of mass fractions, W_1 = 0.003 at temperatures 298.15 K, 303.15 K and 308.15 K.	207
	Table S12. Apparent molar volume (ϕ_V), (η_r-1)/$\sqrt{c}$ and Molar Refraction (R_M) of aqueous pure (Dyphylline + β-CD + H_2O) system in aqueous β-CD solutions of mass fractions, W_1 = 0.005 at temperatures 298.15 K, 303.15 K and 308.15 K.	208
	Table S13. A detailed operation procedure for theoretical calculations.	209
	Table 1: Details of Name, Attribution, CAS Number and Mass Fraction of Materials Studied.	233
	Table 2: Limiting molar volume (ϕ_V^0), viscosity-*B* and viscosity-*A* co-efficient and Molar Refraction (R_M^0) of (L-ALANINE + CDP + H_2O) and (L-VALINE + CDP + H_2O) systems in aqueous CDP solutions of mass fractions, w_1 = 0.001, 0.003, 0.005 at temperatures 298.15 K, 303.15 K and 308.15 K and atmospheric pressure 0.1 MPa.	233-234
	Table 3: Values of various coefficients of equation-3 for L-Alanine and L-Valine in different mass fraction (w_1) of aqueous CDP mixtures.	235
	Table 4: Values of $(\delta\phi_E^0/\delta T)_P$ for L-Alanine and L-Valine in different mass fraction (w) of aqueous CDP mixtures at 298.15 K, 303.15 K and 308.15 K and atmospheric pressure 0.1 MPa.	235

CHAPTERS	TABLES	PAGE NO.
CHAPTER VIII	Table 5: Values of $B/\ \phi_V^0$ for L-Alanine and L-Valine in different mass fraction (w_1) of aqueous CDP mixtures at different temperatures and atmospheric pressure 0.1 MPa.	235
	Table 6: Values of $(\bar{V}_1^0 - \bar{V}_2^0)$, $\Delta\mu_1^{0\neq}$, $\Delta\mu_2^{0\neq}$, $T\Delta S_2^{0\neq}$ and $\Delta H_2^{0\neq}$ for L-Alanine and L-Valine in different mass fraction (w_1) of aqueous CDP mixtures at three different temperatures and atmospheric pressure 0.1 MPa.	236
	Table 7. Limiting Slopes ($\partial\sigma/\partial m$) of the Surface Tension of the Aqueous Solutions of α-Amino Acids.	236
	Table 8: *ΔH°(kJ/mole); ΔG°(kJ/mole) and ΔS°(kJ/mole)* for (a) L-Alanine-CDP (anionic) (b) L-Valine-CDP (anionic) forms in water medium.	237
	Table S1. Density (ρ), Viscosity (η), Refractive index (n_D) of aqueous pure CDP solutions of mass fractions, W_1 = 0.001, 003, 0.005 at temperatures 298.15 K, 303.15 K and 308.15 K and atmospheric pressure 0.1 MPa.	237
	Table S2. Density (ρ), Viscosity (η), Refractive index (n_D) of aqueous pure (L-ALANINE + CDP + H_2O) and (L-VALINE + CDP + H_2O) systems in aqueous CDP solutions of mass fractions, W_1 = 0.001 at temperatures 298.15 K, 303.15 K and 308.15 K and atmospheric pressure 0.1 MPa.	237-238
	Table S3. Density (ρ), Viscosity (η), Refractive index (n_D) of aqueous pure (L-ALANINE + CDP + H_2O) and (L-VALINE + CDP + H_2O) systems in aqueous CDP solutions of mass fractions, W_1 = 0.003 at temperatures 298.15 K, 303.15 K and 308.15 K and atmospheric pressure 0.1 MPa.	239
	Table S4. Density (ρ), Viscosity (η), Refractive index (n_D) of aqueous pure (L-ALANINE + CDP + H_2O) and (L-VALINE + CDP + H_2O) systems in aqueous CDP solutions of mass	240

CHAPTERS	TABLES	PAGE NO.
	fractions, W_1 = 0.005 at temperatures 298.15 K, 303.15 K and 308.15 K and atmospheric pressure 0.1 MPa.	
	Table S5. Apparent molar volume (ϕ_V), (η_r-1)/$\sqrt{m}$ and Molar Refraction (R_M) of aqueous pure (L-ALANINE + CDP + H_2O) and (L-VALINE + CDP + H_2O) systems in aqueous CDP solutions of mass fractions, W_1 = 0.001 at temperatures 298.15 K, 303.15 K and 308.15 K and atmospheric pressure 0.1 MPa.	241-242
	Table S6. Apparent molar volume (ϕ_V), (η_r-1)/$\sqrt{m}$ and Molar Refraction (R_M) of aqueous pure (L-ALANINE + CDP + H_2O) and (L-VALINE + CDP + H_2O) systems in aqueous CDP solutions of mass fractions, W_1 = 0.003 at temperatures 298.15 K, 303.15 K and 308.15 K and atmospheric pressure 0.1 MPa.	242-243
	Table S7. Apparent molar volume (ϕ_V), (η_r-1)/$\sqrt{m}$ and Molar Refraction (R_M) of aqueous pure (L-ALANINE + CDP + H_2O) and (L-VALINE + CDP + H_2O) systems in aqueous CDP solutions of mass fractions, W_1 = 0.005 at temperatures 298.15 K, 303.15 K and 308.15 K and atmospheric pressure 0.1 MPa.	244-245
	Table S8. Molar conductivities of (L-ALANINE + CDP +H_2O) and (L-VALINE + CDP +H_2O) systems in aqueous CDP solutions of mass fractions, W_1 = 0.001, 003, 0.005 at temperatures 298.15 K, 303.15 K and 308.15 K and atmospheric pressure 0.1 MPa.	245-246
	Table S9. Surface Tension σ of L-Alanine and L-Valine as a function of different mass fraction (w_1) of aqueous CDP solutions at temperatures 298.15 K and atmospheric pressure 0.1 MPa.	247

LIST OF FIGURES

CHAPTERS	FIGURES	PAGE NO.
CHAPTER I	**Figure 1:** Diagram showing a host-guest supramolecular inclusion complex.	2
CHAPTER II	**Figure 1:** Hydrophobic interaction brings the interacting molecules closer.	11
	Figure 2: Diagram of Van der Waals forces between molecules.	12
	Figure 3: Illustration of hydrogen bonding in water molecules.	12
	Figure 4: Illustration of electrostatic forces between charged species.	13
	Figure 5: Illustration of ion-dipolar attraction between an ion and polar molecules.	13
	Figure 6: Diagram showing dipole-dipole attraction between polar molecules.	14
	Figure 7: Diagram showing the structure of an NMR instrument.	15
	Figure 8: Diagram of a Fourier Transform Infrared (FTIR) spectrophotometer.	17
	Figure 9: Diagram showing the structure of a UV-visible spectrophotometer.	19
	Figure 10: Diagram showing the working principle of DSC.	20
	Figure 11: Diagram of a TGA instrument.	21
	Figure 12: Illustration showing the working principle of PXRD.	21
	Figure 13: Illustration showing the working principle of SEM.	22
	Figure 1. Job plots of the (a) TZ-α-CD and (b) TZ-β-CD systems.	70

CHAPTERS	FIGURES	PAGE NO.
	Figure 2. Spectra for the generation of Job plots of (a) TZ-α-CD and (b) TZ-β-CD systems.	70
	Figure 3. Variations in the surface tension of the aqueous TZ with increasing concentration of (a) α-CD and (b) β-CD.	71
	Figure 4. Variations in the conductance of the aqueous TZ with increasing concentration of (a) α-CD and (b) β-CD.	71
	Figure 5. Absorption spectra of TZ (35 μM) in various concentration of aqueous (a) α-CD and (b) β-CD in μM respectively.	72
	Figure 6. SEM images of (a) α-CD, (b) β-CD, (c) TZ, (d) TZ-α-CD IC and (e) TZ-β-CD IC.	72
	Figure 7. UV-Vis spectra of (a) TZ, (b) TZ-α-CD and (c) TZ-β-CD at different concentration of CT-DNA.	73
	Figure 8. Time dependent UV-Vis spectra of (a) TZ, (b) TZ+α-CD IC and (c) TZ+β-CD IC under Fenton reaction and (d) percentage of degradation of each component under Fenton process.	74
	Figure 9. Time dependent UV-Vis spectra of (a) TZ, (b) TZ-α-CD IC and (c) TZ-β-CD IC under Photo-Fenton reaction and (d) percentage of degradation of each component under Photo-Fenton process.	75
	Figure 10: Cell viability at different concentration of TZ, TZ-α-CD and TZ-β -CD.	76
	Figure 11. Geometry optimization of the molecules at M06-2X-/6-31+G(d) level of theory. Top and side views of the (a) TZ-α-CD and (b) TZ-β-CD inclusion complex red, gray, white, and blue colour represents oxygen, carbon, hydrogen, and nitrogen atoms respectively.	77
CHAPTER IV	**Figure 12.** LUMO and HOMO plots of (a) TZ-α-CD and (b) TZ-β -CD inclusion complexes.	78

CHAPTERS	FIGURES	PAGE NO.
	Figure 13. Electrostatic potential Maps for (a) TZ-α-CD and (b) TZ-β -CD inclusion complexes.	79
	Figure 14. Plots of reduced density gradient (RDG) against electron density multiplied by the sign of the second Hessian eigenvalue (sign(λ2)ρ(r)) for the (a)TZ-α-CD and (b) TZ-β -CD inclusion complex.	79
	Figure S1. ^{1}H NMR spectra of TZ.	80
	Figure S2. ^{1}H NMR spectra of α-CD.	80
	Figure S3. ^{1}H NMR spectra of β-CD.	81
	Figure S4. ^{1}H NMR spectra of α-CD-TZ IC.	81
	Figure S5. ^{1}H NMR spectra of β-CD-TZ IC.	82
	Figure S6. FTIR spectra of TZ, α-CD and TZ-α-CD.	82
	Figure S7. FTIR spectra of β-CD and TZ-β-CD.	83-84
	Figure S8. Benesi-Hildebrand double reciprocal plot for the effect of *α*-CD and β-CD on the absorbance of TZ (428 nm) at 298.15 K (X axis = 1/[CD] and Y axis = 1/ΔA).	84
	Figure S9. UV-Vis spectra of CT-DNA in presence of different concentration of TZ	85
	Figure S10. Bar diagram representing the percentage of Degradation of pure TZ, TZ-α-CD and TZ-β-CD under Fenton and Photo-Fenton processes within 40 and 16 minutes respectively at 298.15 K.	85
	Figure 1: Generation of Job plot **(a)** spectra and **(b)** the obtained Job plot.	115
	Figure 2: Variations in the surface tension of the 6-MP with increasing concentration of **(a)** β-CD.	116
	Figure 3: Absorption spectra of 6-MP (40 μM) in various concentrations of aqueous **(a)** β-CD in μM.	116

CHAPTERS	FIGURES	PAGE NO.
	Figure 4: ^{1}H NMR spectra of **(a)** β-CD, **(b)** 6-MP, and **(c)** IC	117
	Figure 5: FTIR spectra of 6-MP, β-CD, and 6-MP-β-CD IC.	118
	Figure 6: Top and side viewsof the optimized geometries for the 6-MP-β-CD complex at M06-2X/6-31+G(d) level of theory. Red, gray, white, blue and yellow color represents oxygen, carbon, hydrogen, nitrogen and sulfur atoms respectively.	119
	Figure 7: SEM images of **(a)** β-CD, **(b)** 6-MP, and their **(c)** IC.	119
	Figure 8: PXRD spectra of β-CD, 6-MP and its IC.	120
	Figure 9: DSC thermograms of β-CD, 6-MP and its IC.	121
	Figure 10: (a) TGA of β-CD, 6-MP and its IC.	121
	Figure 11: UV-spectra of 6-MP+β-CD of different concentrations (mg.mL^{-1}) in aqueous medium **(a)** 0.033, **(b)** 0.066, **(c)** 0.099, **(d)** 0.132, **(e)** 0.165, **(f)** 0.198, and **(g)** 0.228.	122
CHAPTER V	**Figure 12:** Time-dependent UV-Vis spectra of **(a)** 6-MP, **(b)** IC and **(c)** percentage of degradation of each component under sunlight.	122
	Figure 13: UV-Vis spectra of **(a)** 6-MP **(b)** IC at different concentrations of CT-DNA.	123
	Figure 14: IC and 6-MP cytotoxicity percentages at various concentrations.	123
	Figure 15: HOMO and LUMO charge densities of the6-MP-β-CD complex.	124
	Figure 16: Electrostatic potential maps for the 6-MP-β-CD complex.	124
	Figure 17: Plots of reduced density gradient (RDG) for 6-MP-β-CD complex.	125

CHAPTERS	FIGURES	PAGE NO.
	Figure S1: Molecular structures of **(a)** Beta Cyclodextrin and **(b)** 6-Mercaptopurine monohydrate.	125-126
	Figure S2: Pictures with Ampicillin as positive controls and sterile distilled water as negative controls in case of **(a)** *E.Coli*. and **(b)** *B. subtilis*.	126
	Figure S3: Benesi-Hildebrand double reciprocal plot for the effect of β-CD on the absorbance of TZ (324 nm) at 298.15 K (X axis = 1/[CD] and Y axis = 1/ΔA).	127
	Figure S4: DTG thermograms of β-CD, 6-MP and its IC.	127
	Figure S5: UV-Vis spectra of saturated concentration of IC.	128
	Figure S6: UV-Vis spectra of CT-DNA in presence of different concentration of 6-MP.	128
	Figure S7: Well diffusion assay of 6-MP and β-CD, singly and in combination together as IC.	129
CHAPTER VI	**Figure 1: (a)** Spectra for generation of Job plot and **(b)** the generated Job plot.	151
	Figure 2: (a) Absorption spectra of BPA with various concentrations of β-CD and **(b)** Double reciprocal Benesi- Hildebrand plot.	151
	Figure 3: ^{1}H NMR spectra of **(a)** β-CD, **(b)** BPA and **(c)** IC.	152
	Figure 4: Solid-state FTIR spectra of β-CD, BPA and IC.	153
	Figure 5: SEM morphologies of **(a)** β-CD, **(b)** BPA and **(c)** IC.	153
	Figure 6: (a) PXRD patterns and **(b)** DSC thermograms of BPA, β-CD and IC.	154
	Figure 7: (a) TGA and **(b)** DTA thermograms of BPA, β-CD and IC.	154

CHAPTERS	FIGURES	PAGE NO.
	Figure 8: UV-Vis spectra of **(a)** BPA and **(b)** IC in presence of different concentrations of CT-DNA.	155
	Figure 9: Ground state geometry for the BPA-β-CD complex at M06-2X/6-31+G(d) level of theory. Here red, gray, and white colours represent oxygen, carbon, and hydrogen atoms respectively.	155
	Figure 10: HOMO and LUMO charge densities of BPA-β-CD complex.	156
	Figure 11: (a) Electrostatic potential maps and **(b)** Plots of reduced density gradient (RDG) for BPA-β-CD inclusion complex.	156
	Figure 12: Zone of inhibition of BPA and IC (in different concentrations) against the studied microorganism (the black line above the column represents the standard deviation of triplicate determination).	157
	Figure 13: Antimicrobial activity of BPA (A, C, E) and IC (B,D,F) against *S. typhimurium* (A,B), *S. flexneri* (C,D) and *E. coli* (E,F) (Concentration of the sample applied i=20mM, ii=10 mM, iii=5mM).	158
	Figure 14: Antimicrobial activity of BPA (G,I) and IC (H,J) against *S. aureus* (G,H) and *B. megaterium* (I,J) (Concentration of the sample applied i=20mM, ii=10 mM, iii=5mM).	159
	Figure 1: Variation of surface tension of aqueous Dyphylline- β-CD system at 298.15 K.	182
	Figure 2: (a) Job plot (b) spectra of aqueous Dyphylline-β-CD system at λ_{max} = 206 nm at 298.15 K.	182
	Figure 3: ^{1}H-NMR spectra of pure Host (β-CD), Guest (Dyphylline) and IC. Figure 3. B reprinted with permission from ref 24. Copyright 2022 Elsevier.	183

CHAPTERS	FIGURES	PAGE NO.
CHAPTER VII	**Figure 4:** SEM imageries of (a) β-CD, (b) Dyphylline and (c) IC.	184
	Figure 5: Time-dependent UV-Vis spectra of (a) Dyphylline, (b) IC and (c) percentage of degradation of each component under sunlight.	184
	Figure 6: Optimized geometries for the Dyphylline-β-CD complex at M06-2X/6-31+G (d) level of theory (a), (b) side views and (c) top view.	185
	Figure 7: HOMO and LUMO charge densities of Dyphylline-β-CD complex.	185
	Figure 8: Antimicrobial activity of IC (i,iv), β-CD (iii,v) and Dyphylline (iii,vi) against *B. subtilis* (i,ii,iii) and *B. megaterium* (iv,v,vi) (Concentration of the sample applied a=20 mM, b=10 mM, c=5 mM).	186
	Figure 9: Antimicrobial activity of IC (i,iv), β-CD (iii,v) and Dyphylline (iii,vi) against *S. typhimurium* (i,ii,iii) and *E. coli* (iv,v,vi) (Concentration of the sample applied a=20 mM, b=10 mM, c=5 mM).	187
	Figure 10: Percentage of cytotoxicity of Dyphylline and IC at different concentration.	188
	Figure S1: Variation of conductivity of aqueous Dyphylline-β-CD system at 298.15 K.	188
	Figure S2: (a) Absorption spectra of Dyphylline (40 μM) in various concentrations of aqueous β-CD.	189
	Figure S3. Benesi-Hildebrand double reciprocal plot for the effect of β-CD on the absorbance of Dyphylline (206 nm) at 298.15 K (X axis = 1/[CD] and Y axis = 1/ΔA).	189
	Figure S4: ^{1}H NMR spectra of (a) β-CD, (b) Dyphylline and (c) IC with normal and zoomed version with all chemical shifts.	190-191

CHAPTERS	FIGURES	PAGE NO.
	Figure S5: Plot of ϕ_V^0 versus mass fraction (w_1) of aqueous β-CD solutions and as a function of temperature (T/K).	191
	Figure S6: B plotted as a function of temperature (T/K) and different mass fractions (w_1) of aqueous β-CD solutions.	192
	Figure S7: Plot of limiting molar refractive index (R_M^0) as a function of different mass fractions (w_1) of aqueous β-CD solutions and as a function of temperature (T/K).	192
	Figure S8: UV-Vis absorbance spectra of (a) Dyphylline (b) IC at different concentrations of CT-DNA; (c) and (d) are the CT-DNA spectra at various concentrations of Dyphylline and IC respectively.	193
	Figure S9: Electrostatic potential maps for Dyphylline-β-CD complex.	194
	Figure S10: Plots of reduced density gradient (RDG) for Dyphylline-β-CD complex.	194
	Figure S11: Antimicrobial activity of IC (i), β-CD (ii) and Dyphylline (iii) against *S. aureus* (Concentration of the sample applied a=20 mM, b=10 mM, and c=5 mM).	195
	Figure 1: Plot of ϕ_V^0 as a function of different mass fraction (w_1) of aqueous CDP solutions and as a function of temperature (T/K).	226
	Figure 2: Plot of B as a function of different mass fraction (w_1) of aqueous CDP solutions and as a function of temperature (T/K).	226
	Figure 3: Plot of limiting molar refractive index (R_M^0) as a function of different mass fraction (w_1) of aqueous CDP solutions and as a function of temperature (T/K).	227

CHAPTERS	FIGURES	PAGE NO.
CHAPTER VIII	**Figure 4:** Plot of molar conductance as a function of concentration of Amino acids in different mass fraction (w_1) of aqueous CDP in solutions at 298.15 *K*.	227
	Figure 5: Plot of molar conductance as a function of concentration of Amino acids in different mass fraction (w_1) of aqueous CDP in solutions at 303.15 *K*.	228
	Figure 6: Plot of molar conductance as a function of concentration of Amino acids in different mass fraction (w_1) of aqueous CDP in solutions at 308.15 *K*.	228
	Figure 7: Plot of Surface Tension σ of L-Alanine and L-Valine as a function of different mass fraction (w_1) of aqueous CDP solutions.	229
	Figure 8: ^{1}H-NMR spectra of pure CDP (Pic. 1), L-Alanine (Pic. 2) and L-Valine (Pic. 3) in D_2O.	229-230
	Figure 9: ^{1}H-NMR spectra of L-Alanine + CDP (Pic. 4) and L-Valine + CDP (Pic. 5) in D_2O.	230-231
	Figure 10. Optimized geometries for the (a) L-Alanine-CDP (neutral) (b) L-Valine-CDP (neutral) (c) L-Alanine-CDP (anionic) (d) L-Valine-CDP (anionic).	232
	Figure 11: Electrostatic potential maps for (a) L-Alanine-CDP (anionic) (b) L-Valine-CDP (anionic) forms.	232
	Figure 12: Plots of reduced density gradient (RDG) against electron density multiplied by the sign of the second Hessian eigenvalue (sign(λ2)ρ(r)) for (a) L-Alanine-CDP (b) L-Valine-CDP systems.	233

LIST OF SCHEMES

CHAPTERS	SCHEMES	PAGE NO.
CHAPTER IV	**Scheme 1.** Molecular structure of Tartrazine (TZ), Alpha Cyclodextrin(α-CD), and Beta Cyclodextrin(β-CD).	97
CHAPTER VI	**Scheme 1:** Molecular structures of (a) β-CD, (b) BPA and (c) Cone-like structure of β-CD.	162
CHAPTER VII	**Scheme 1:** Molecular structures of Beta-Cyclodextrin and Dyphylline.	209
	Scheme 2: Structures of β-CD and Dyphylline.	209
	Scheme 3: Plausible mode of insertion of Dyphylline insight into β-CD.	210
CHAPTER VIII	**Scheme 1:** The molecular structure of Chloroquine diphosphate, L-Alanine and L- Valine.	248
	Scheme 2: Plausible interaction that takes place in between CDP drug and Amino acids.	248-249

ABBREVIATIONS

TERMS	FULL FORMS
CD	**Cyclodextrin**
α-CD	**α-cyclodextrin**
β-CD	**β-cyclodextrin**
IC	**Inclusion complex**
TZ	**Tartrazine**
6-MP	**6-Mercaptopurine Monohydrate**
BPA	**Bisphenol A**
CDP	**Chloroquin Diphosphate**
AA	**Amino acid**
CT-DNA	**Calf Thymus DNA**
DPPH	**2,2-Diphenyl-1-Picrylhydrazyl**
DPBF	**1,3-Diphenylisobenzofuran**
µm	**Micrometre**
Å	**Angstrom**
cm	**Centimetre**
DMF	**Dimethylformamide**
DMSO	**Dimethyl sulfoxide**
EtOH	**Ethanol**
Eq.	**Equation**
eV	**Electron Volt**
Fig.	**Figure**
g	**Gram**

hrs	**Hours**
Hz	**Hertz**
FTIR	**Fourier Transform Infrared spectroscopy**
K	**Kelvin**
M	**Molar**
m	**Meter**
mg	**Milligram**
min	**Minute**
mL	**Millilitre**
µM	**Micromolar**
µL	**Microlitre**
NIR	**Near Infrared**
^{o}C	**Degree Celsius**
pH	**Potential of Hydrogen**
rpm	**Revolutions Per Minute**
SEM	**Scanning Electron Microscopy**
TGA	**Thermogravimetric Analysis**
DSC	**Differential Scanning Calorimetry**
UV-vis	**Ultraviolet-visible**
NMR	**Nuclear Magnetic Resonance**
XRD	**X-Ray Diffraction**
AOP	**Advanced Oxidation Process**
MTT	**(3-[4,5-dimethylthiazol-2-yl]-2,5 diphenyl tetrazolium bromide)**
$ABTS^{+}$ cation(s)	**(2′-azino-bis(3-ethylbenzothiazoline-6-sulfonic acid) radical**
FRAP	**Ferric reducing antioxidant power**

LIST OF APPENDICES

APPENDIX A	List of Publications
APPENDIX B	List of Seminars/Conferences Attended

APPENDIX A

LIST OF PUBLICATIONS

As First Author

1. **Cyclic oligosaccharides as controlled release complexes with food additives (TZ) for reducing hazardous effects**

ELSEVIER

Journal of Molecular Liquids, 2022, 348, 118429

(Included in the Thesis)

2. **Exploring inclusion complex of an anti-cancer drug (6-MP) with ß-cyclodextrin and its binding with CT-DNA for innovative applications in anti-bacterial activity and photostability optimized by computational study**

ROYAL SOCIETY OF CHEMISTRY

RSC Advances, 2022, 22(48), 30936-30951

(Included in the Thesis)

3. Assembled Bisphenol A with cyclic oligosaccharide as the controlled release complex to reduce risky effects

Springer

Environmental Science and Pollution Research, 2023, 30(15), 43300-43319

(Included in the Thesis)

4. Probing the molecular assembly of a metabolizer drug with β-cyclodextrin and its binding with CT-DNA in augmenting antibacterial activity and photostability by physicochemical and computational methodologies

ACS OMEGA

ACS Chemistry for Life®

ACS Omega, 2022, 7(30), 26211-26225

(Included in the Thesis)

5. Investigation of molecular interactions insight into some biologically active amino acids and aqueous solutions of an anti-malarial drug by physicochemical and theoretical approach

ELSEVIER

Journal of Molecular Liquids, 2021, 341, 116933

(Included in the Thesis)

6. **Subsistence of diverse interactions of some biologically important molecules in aqueous ionic liquid solutions at various temperatures by experimental and theoretical investigation**

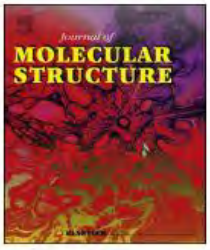

Journal of Molecular Structure, 2022, 1257, 132571

7. **A combined physicochemical and computational investigation of the inclusion behaviour of 3-(1-Naphthyl)-D-alanine Hydrochloride insights into b-Cyclodextrin**

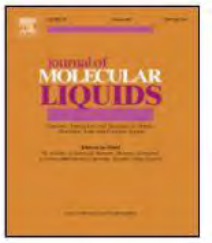

Journal of Molecular Liquids, 2023, 378, 121583

As Co-Author

8. **Green synthesis and characterization of heterostructure MnO-FeO nanocomposites to study the effect on oxidase enzyme mimicking, HSA binding interaction and cytotoxicity**

Chemical Physics Letter, 2021, 1225, 129093

9. Synthesis and characterization of $Mo_xFe_{1-x}O$ nanocomposites for the ultra-fast degradation of methylene blue via a Fenton-like process: a green approach

ROYAL SOCIETY OF CHEMISTRY

New Journal of Chemistry, 2022, 46, 18055-18068

10. Rational Synthesis and Characterization of Temperature Switching $ZnFe_2O_4$/ZnO Nanocomposite Used for Anti-bacterial, Anti-oxidant and Seed Germination Properties

ROYAL SOCIETY OF CHEMISTRY

New Journal of Chemistry, 2024, 48, 3624-3637

11. Green synthesized copper assisted iron oxide nanozyme for the efficient elimination of industrial pollutant *via* peroxodisulfate activation

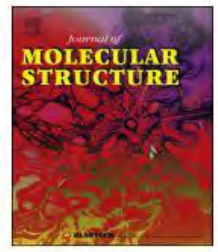

ELSEVIER

Journal of Molecular Structure, 2023, 1283, 135267

12. β-Cyclodextrin-Stabilized Biosynthesis Nanozyme for Dual Enzyme Mimicking and Fenton Reaction with a High Potential Anticancer Agent

ACS Omega, 2022, 7(5), 4457-4470

13. Molecular interactions of some bioactive molecules prevalent in aqueous ionic liquid solutions at different temperatures investigated by experimental and computational contrivance

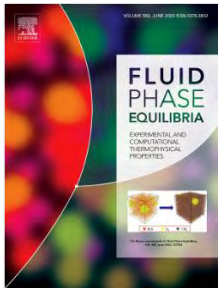

Fluid Phase Equilibria, 2022, 557, 113415

14. Assemble multi-enzyme mimic tandem Mn_3O_4@ g-C_3N_4 for augment ROS elimination and label free detection

Chemical Engineering Journal, 2023, 463, 142355

15. Exploring Various Molecular Interactions of Two Essential Amino Acids Prevalent in Aqueous Solutions of an Ionic Liquid by Density, Viscosity, Refractive Index, Conductance, Surface Tension, Nuclear Magnetic Resonance, Ultraviolet, and Computational Studies

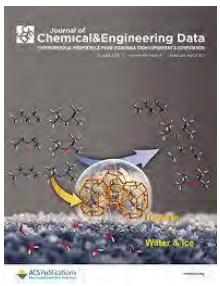

Journal of Chemical and Engineering Data, 2023, 68(12), 3045-3061

16. Exploring Brilliant Blue FCF Assembly with Beta Cyclodextrin, Characterizations and Applications in Biological Systems Using Physicochemical and Computational Methods

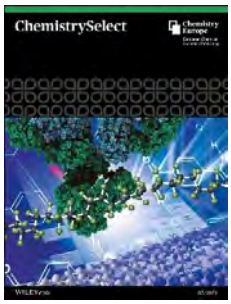

ChemistrySelect, 2024, 9(2), e202302895

17. Exploring Diverse Amino Acid-Polyol Interactions Prevailing in Aqueous Systems at Different Temperatures by Physicochemical Contrivance Simultaneously Optimized by DFT

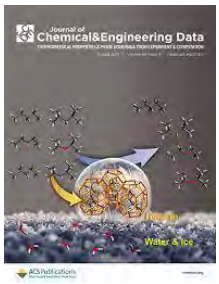

Journal of Chemical and Engineering Data, 2024, 69(4), 1468-1483

18. Physicochemical studies of some bioactive molecules in aqueous solution of tetrabutylammonium methanesulphonate (TBAMS) to investigate assorted molecular interaction at different temperatures simultaneously optimized by computational approach

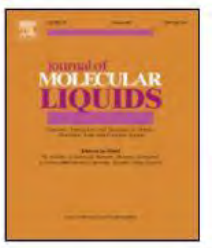

Journal of Molecular Liquids, 2024, 395, 123818

19. Physicochemical and computational investigations of some essential amino acids prevailing in aqueous solutions of a food preservative (SBz) with the manifestation of hydrophobic and hydrophilic interactions at different temperatures

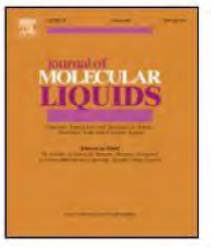

ELSEVIER

Journal of Molecular Liquids, 2024, 408, 125238

---

20. Physicochemical contrivance for exploring host-guest inclusion complex of a significant green solvent with a cyclic oligosaccharide and its innovative application optimized by computational approach

DE G DE GRUYTER

Zeitschrift für Physikalische Chemie, (ahead-of-print), 2023

---

21. Multienzyme Mimicking Cascade Mn_3O_4 Catalyst to Augment Reactive Oxygen Species Elimination and Colorimetric Detection: A Study of Phase Variation upon Calcination Temperature

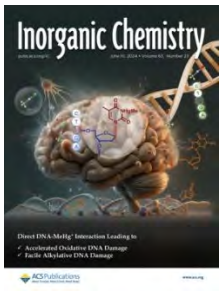

ACS Chemistry for Life®

Inorganic Chemistry, 2024, 63(23), 10542-10556

---

22. Phase variation of manganese oxide in the MnO@ZnO nanocomposite with calcination temperature and its effect on structural and biological activities

SCIENTIFIC REPORTS

SPRINGER NATURE

Scientific Reports, 2023, 13, 21542

23. Label-Free Detection of Epinephrine Using Flower-like Biomimetic CuS Antioxidant Nanozymes

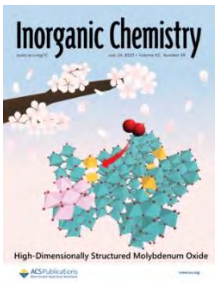

ACS Chemistry for Life®

Inorganic Chemistry, 2023, 62(29), 11291–11303

24. A Physicochemical Approach to Explore the Host Guest Inclusion Complex of β-Cyclodextrin with an Ionic Liquid ([C4mpy] Cl) in Aqueous Media

B P International

(Book Chapter)

Progress in Chemical Science Research, 2023, 4, 1-16

APPENDIX B

LIST OF SEMINARS/CONFERENCES ATTENDED

Sl. No.	Seminar/Conference	Date/Year	Organizer and Venue	Role
(1)	National Conference on "Environmental Determinism, Diverse Pollutions, Sources, and Controlling Management through Sciences and Humanities"	March 22-23, 2021	Alipurduar University	Oral Presentation
(2)	National Seminar on "Frontiers in Chemistry-2020"	March 5, 2020	Department of Chemistry, University of North Bengal	Poster Presentation
(3)	International Seminar on Frontiers in Chemistry 2023 & Prof. C. N. R. Rao Endowment Lecture	March 13-15, 2023	Department of Chemistry, University of North Bengal & CRSI North Bengal Local Chapter	Oral Presentation
(4)	International Conference on Advances in Plants, Microbes and Agricultural Sciences	March 2-4, 2023	DST (FIST) & UGC- SAP Assisted DRS & Department of Chemistry, University of North Bengal	Oral Presentation